International Journal of Nanomedicine

Dovepress
open access to scientific and medical research

Open Access Full Text Article

ORIGINAL RESEARCH

Essential oil-loaded lipid nanoparticles for wound healing

This article was published in the following Dove Press journal:
International Journal of Nanomedicine

Francesca Saporito[1]
Giuseppina Sandri[1]
Maria Cristina Bonferoni[1]
Silvia Rossi[1]
Cinzia Boselli[1]
Antonia Icaro Cornaglia[2]
Barbara Mannucci[3]
Pietro Grisoli[1]
Barbara Vigani[1]
Franca Ferrari[1]

[1]Department of Drug Sciences, University of Pavia, Pavia, [2]Department of Public Health, Experimental and Forensic Medicine, University of Pavia, Pavia, [3]Centro Grandi Strumenti, University of Pavia, Pavia, Italy

Abstract: Chronic wounds and severe burns are diseases responsible for severe morbidity and even death. Wound repair is a crucial process and tissue regeneration enhancement and infection prevention are key factors to minimize pain, discomfort, and scar formation. The aim of this work was the development of lipid nanoparticles (solid lipid nanoparticles and nanostructured lipid carriers [NLC]), to be loaded with eucalyptus or rosemary essential oils and to be used, as medical devices, to enhance healing of skin wounds. Lipid nanoparticles were based on natural lipids: cocoa butter, as solid lipid, and olive oil or sesame oil, as liquid lipids. Lecithin was chosen as surfactant to stabilize nanoparticles and to prevent their aggregation. The systems were prepared by high shear homogenization followed by ultrasound application. Nanoparticles were characterized for physical–chemical properties, bioadhesion, cytocompatibility, in vitro proliferation enhancement, and wound healing properties toward normal human dermal fibroblasts. Antimicrobial activity of nanoparticles was evaluated against two reference microbial strains, one of *Staphylococcus aureus*, the other of *Streptococcus pyogenes*. Finally, the capability of nanoparticles to promote wound healing in vivo was evaluated on a rat burn model. NLC based on olive oil and loaded with eucalyptus oil showed appropriate physical–chemical properties, good bioadhesion, cytocompatibility, in vitro proliferation enhancement, and wound healing properties toward fibroblasts, associated to antimicrobial properties. Moreover, the in vivo results evidenced the capability of these NLC to enhance the healing process. Olive oil, which is characterized by a high content of oleic acid, proved to exert a synergic effect with eucalyptus oil with respect to antimicrobial activity and wound repair promotion.

Keywords: lipid nanoparticles, eucalyptus essential oil, antimicrobial properties, wound healing

Introduction

Wound repair is one of the most complex physiologic processes, involving a multitude of different cell types, the contribution of which is tightly regulated over time. The breakdown of such a complex path could result in wound healing failure, leading to nonhealing wounds. The typical path of wound repair includes overlapping stages of inflammation, new tissue generation, and subsequent remodeling of neoformed tissue. These stages take place over dramatically different timescales, lasting from minutes (initial clotting and coagulation) to several months or even years.[1,2]

Chronic wounds (including venous leg ulcers, diabetic foot ulcers, arterial insufficiency, and pressure ulcers) determine severe morbidity and even mortality especially in older individuals, in particular those affected from diabetes mellitus and vascular diseases. In addition, surgery, more common in older population, presents risk of wound complication. In general, chronic wounds deeply affect quality of life and wound care requires high costs of therapy.[3]

Correspondence: Giuseppina Sandri
Department of Drug Sciences, University of Pavia, Viale Taramelli 12, 27100 Pavia, Italy
Tel +39 038 298 7728
Fax +39 038 242 2975
Email giuseppina.sandri@unipv.it

submit your manuscript | www.dovepress.com
Dovepress
http://dx.doi.org/10.2147/IJN.S152529

Resident cells are less proliferating in chronic wounds and possess a morphology similar to that of senescent cells. In particular, fibroblasts of chronic wounds (long-lasting vascular leg ulcers) are characterized by a poorer response to platelet-derived growth factor, altered capability of transforming growth factor beta type II receptor expression, and abnormal phosphorylation of critical signal transduction proteins. Such features are typical of cells exposed to low oxygen tension, suggesting that chronic wounds are hypoxic.[3]

The effect of microbial burden on healing of chronic wound is not completely understood and it is probably underestimated.[2] The presence of a biofilm was indicated as a critical factor and a correlation between depth and duration of the lesion and the presence of *Staphylococcus* strains was demonstrated.[4] Moreover, microbial wound colonization (typically due to *Staphylococcus aureus, Pseudomonas aeruginosa, Streptococcus pyogenes*, and some *Clostridium* strains) was proved responsible for a further delay in wound recovery.[5]

Burns are skin wounds that can affect a significant portion of the body. Prevention of microbial infection and scar formation are key factors for wound healing.[6]

Many efforts to enhance the effectiveness of wound healing process have been focused on boosting the antimicrobial activity of topically applied devices, preventing infections, promoting tissue regeneration, and minimizing pain, discomfort, and scar formation.

In the last decades, the occurrence of multiresistant bacteria poses a serious problem worldwide, making a challenge the choice of appropriate treatment for patients affected with infected lesions.[7]

Natural products including β-glucans, aloe, honey, and especially essential oils (EOs) have been proposed as antibacterial agents.[8] In particular, EOs are known to possess antimicrobial effect against multiresistant bacteria, thanks to a broad spectrum of biologic and antimicrobial activity.[9]

EOs are volatile products produced by the secondary metabolism of plants, are extracted from nonwoody part (flowers, seeds, leaves, fruits, and roots), and are mainly composed of terpenes and terpenoids and aromatic and aliphatic constituents.[10]

Eucalyptus leaf extracts (EO from eucalyptus tree, belonging to the family of Myrtaceae) demonstrated various biologic effects, such as antibacterial, antifungal, antiseptic, antihyperglycemic, and antioxidant activities; 1,8-cineole or eucalyptol is the most important component, responsible for bioactive properties.[11]

Rosemary EO (from *Rosmarinus officinalis*, belonging to the family of Lamiaceae), which is mainly composed of camphor, 1,8-cineole, borneol, verbenone, α-pinene, and camphene, has been historically used as an antibacterial, antifungal, and antioxidant agent.[12–14]

All EOs are unstable volatile compounds and are easily degradable (by oxidation, volatilization, heating, and light): encapsulation in nanosystems should, therefore, represent a useful tool to enhance their stability and improve antibacterial activity.[15]

Giving these premises, the aim of this work was the development of lipid nanoparticles, solid lipid nanoparticles (SLN), and nanostructured lipid carriers (NLC), to be loaded with eucalyptus or rosemary EOs and to be used, as medical devices, to enhance healing of skin wounds.

Lipid nanoparticles were based on natural lipids: cocoa butter, as solid lipid, and olive oil or sesame oil, as liquid lipids. Lecithin was chosen as surfactant to stabilize nanoparticles and to prevent their aggregation. The systems were prepared by high shear homogenization followed by ultrasound application.

Nanoparticles were characterized for physical–chemical properties, bioadhesion, cytocompatibility, in vitro proliferation enhancement, and wound healing properties toward normal human dermal fibroblasts (NHDF). Antimicrobial activity of nanoparticles was evaluated against two reference microbial strains, one of *Staphylococcus aureus*, the other *of Streptococcus pyogenes*. Finally, the capability of nanoparticles to promote wound healing in vivo was evaluated on a rat burn model.

Materials and methods

Materials

Lipid nanoparticles (SLN or NLC) were prepared by using cocoa butter (Aboca S.p.A., Sansepolcro, Italy) as solid lipid, olive oil (o) (Ph. Eur.) (Sigma-Aldrich, Milan, Italy) or sesame oil (s) (Sigma-Aldrich) as liquid lipids, L-α-phosphatidylcholine (L-α-lecithin) from soybean (Sigma-Aldrich) as surfactant, and eucalyptus globulus oil (e) (Janousek, Milan, Italy, Aboca S.p.A.) or rosemary oil (r) (Sigma-Aldrich) as EOs. Pullulan (pull) (food grade, Hayashibara, Japan, Giusto Faravelli, Milan, Italy) was used as viscosifying agent.

Methods

Lipid nanoparticle preparation

Lipid nanoparticles were prepared by high shear homogenization followed by ultrasound application to avoid agglomeration during cooling.[16,17]

Cocoa butter (225 mg) was used as lipid phase for SLNs, whereas NLCs were based on a lipid phase made of cocoa butter (150 mg) mixed with olive oil (75 mg) or sesame oil (75 mg).

Each lipid phase was melted at 40°C and eucalyptus or rosemary EO (75 mg) was added. The total amounts of lipid components were the same for SLN and NLC.

An aqueous phase (12.5 mL) containing lecithin (150 mg) was heated to 40°C and poured into the lipid phase under homogenization at 24,000 rpm for 5 min with an UltraTurrax equipment (T25, IKA, Labortechnik, Denmark). The resulting emulsion was cooled by diluting with distilled water (12 mL) at 2°C–8°C and subjected to ultrasounds (ultrasound frequency 37 kHz) (Elmasonic S80 H, Elma Hans Schmidbauer GmbH & Co, Singen, Germany) for 10 min, to avoid agglomeration.

The resulting lipid nanoparticle suspension was characterized as such or after addition of pull to obtain 5% w/w as final pull concentration in the lipid nanoparticle suspension. The quali-quantitative composition of all the nanosystems is reported in Table 1.

Lipid nanoparticle characterization

Physical–chemical properties

Particle size (PS) and polydispersity index (PI) of all developed nanosystems were assessed at 25°C by photon correlation spectroscopy (PCS) at an angle of 90° (Beckman Coulter N5, Instrumentation Laboratory, Milan, Italy) after suitable dilution of samples with bidistilled and filtered water (0.22 µm, HA Millipore, Merck KGaA, Darmstadt, Germany).

Physical stability of nanoparticles was evaluated up to 90 days of storage at 2–8°C.

Zeta potential of the more promising formulation was measured at 25°C (Nano ZSP, Malvern Instruments, Alfatest, Rome, Italy).

These nanosystems were also analyzed by a transmission electron microscope (TEM; Jeol JEM-1200 EX II, Basiglio, Milan, Italy) equipped with a TEM CCD camera (Mega View III, Jeol, Basiglio, Italy), after sample deposition on copper grids (Formavar/Carbon 300 mesh, Agar Scientific, Assing, Rome, Italy).

Eucalyptus EO assay

Loading of eucalyptus EO in lipid carriers was determined by means of head space solid phase microextraction (HSSPME) coupled with gas chromatography-mass spectrometry (GC-MS) (according to eucalyptus oil – 07/2010:0390, Eur Ph. 9.0 Ed monograph). The following HSSPME experimental parameters were used: sample amount, 100 µL; water addition, 10 mL; fiber polydimethylsiloxane (100 µm); extraction temperature, 40°C; extraction time, 30 min; desorption temperature, 280°C; desorption time, 5 min.

One hundred-microliter aliquots of eucalyptus EO extracted from lipid nanoparticles and eucalyptus EO dispersed in an aqueous lecithin solution at the same concentration of lipid nanoparticles were separately injected.

GC-MS analysis was effected on a Thermo Scientific DSQII single quadrupole GC-MS system (Thermo Fisher Scientific, Milan, Italy) (Xcalibur MS Software Version 2.1) equipped with a Restek Rtx-5 MS capillary column (30 m, 0.25 mm i.d., 0.25 µm film thickness), according to the following temperature program: 4 min at 60°C, then 10°C/min up to 220°C, held for 10 min; carrier gas helium, 1.0 mL/min; injector temperature, 280°C, splitless mode; transfer line temperature, 250°C; run time, 30 min. All mass spectra were acquired in electron-impact mode with ionization voltage equal to 70 eV; ion source temperature 250°C; acquisition mass range 35–500 Da.

Each sample was analyzed in triplicate. The content percentage of each oil component was computed from the corresponding GC-MS peak area without applying any correction factor.

Bioadhesion measurements

Bioadhesion measurements were carried out using a texture analyzer apparatus (TA.XT plus, Stable Microsystems, ENCO, Spinea, Italy) equipped with a 1 kg load cell, a cylinder probe having a diameter of 10 mm (P10), and the A/MUC

Table 1 Quali-quantitative compositions of all the systems prepared

	Lecithin (mg)	Cocoa butter (mg)	Olive oil (mg)	Sesame oil (mg)	Eucalyptus oil (mg)	Rosemary oil (mg)
SLN b	150	225	–	–	–	–
SLN e	150	225	–	–	75	–
SLN r	150	225	–	–	–	75
NLC o/b	150	150	75	–	–	–
NLC s/b	150	150	–	75	–	–
NLC o/e	150	150	75	–	75	–
NLC o/r	150	150	75	–	–	75
NLC s/b	150	150	–	75	–	–
NLC s/e	150	150	–	75	75	–
NLC s/r	150	150	–	75	–	75

Abbreviations: SLN, solid lipid nanoparticles; NLC, nanostructured lipid carriers; b, blank-unloaded; e, eucalyptus oil; r, rosemary oil; o, olive oil; s, sesame oil.

measuring system.[18,19] The A/MUC measuring system consists of a support in which a biologic substrate can be fixed. In this case, the biologic substrate chosen to mimic damaged skin was an egg shell membrane,[18] wetted with 100 µL of isotonic saline (NaCl 0.9% w/v). To recover the membrane, the egg shell was placed in a 0.5 M HCl solution for 1 h. The A/MUC system was thermoset at 32°C. One hundred microliters of each nanosystem containing 5% w/w of pull, as described in the section Lipid nanoparticle preparation, and 5%/w pull solution, as control, were placed onto the cylinder probe covered by filter paper disc and the sample and the biologic substrate were put in contact under a preload of 2.5 N for 3 min.

The cylinder probe was then moved upward at a prefixed speed of 2.5 mm/s up to the complete separation of the bioadhesive interface (egg shell membrane–sample).

The force of detachment was recorded as a function of displacement and the bioadhesion parameter work of adhesion (area under the curve [AUC]) (mN mm, AUC) was calculated as the area under the force vs displacement curve.

The normalized adhesion parameter ΔAUC/AUC was subsequently calculated according to the following equation:

$$\Delta AUC/AUC = (AUC_{bs} - AUC_{blank})/AUC_{blank}$$

where:

AUC_{bs} = work of adhesion obtained in presence of the biologic substrate;

AUC_{blank} = work of adhesion obtained from blank measurements.

Such a normalization should allow comparison of the bioadhesive properties of samples characterized by different cohesive properties (viscosity).[20]

In vitro biocompatibility

Cytotoxicity test

NHDF from juvenile foreskin (PromoCell GmbH, VWR, Milan, Italy) were used. Cells between the second and fifth passage were employed for all the experiments. As growth medium (GM) Dulbecco's Modified Eagle Medium (Lonza, Milan, Italy), supplemented with 10% fetal calf serum (Euroclone, Milan, Italy) and 200 IU/mL penicillin-0.2 mg/mL streptomycin (PBI International, Milan, Italy), was used.

Fibroblasts were seeded in each well of 96-well plates (area 0.34 cm^2) at a density of 10^5 cells/cm^2. Cells were grown for 24 h at 37°C in a 95% air/5% CO_2 atmosphere with 95% relative humidity to obtain subconfluence.

Then cells were washed with saline solution and subsequently put in contact with 200 µL of each sample. Nanoparticle suspensions, as described in the section Lipid nanoparticle preparation, were diluted with GM in a 1/20, 1/40, and 1/100 w/w ratio. In the case of 1/100 dilution, nanoparticle suspensions containing 5% w/w pull, as described in the section Lipid nanoparticle preparation, were also examined and cytocompatibility was compared with that of 5% w/w pull solution diluted 1/100 with GM. Cells kept in contact with GM were considered as positive control (standard growth conditions). After 3 h contact, an MTT test was performed. This test is based on the activity of mitochondrial dehydrogenases of vital cells, which convert MTT to formazan. One hundred twenty-five microliters of MTT solution (Sigma Aldrich) at 0.25 µg/mL concentration in Hank's buffered salt solution pH 7.4 was put in contact with each sample for 3 h. The reagent was then removed from each well and the cells were washed with phosphate-buffered saline (PBS) (150 µL) to remove the samples and the unreacted MTT solution. After PBS removal, 100 µL of dimethyl sulfoxide was put in each well and the absorbance was assayed at 570 nm by means of an enzyme-linked immunosorbent assay plate reader (Imark Absorbance Reader, Biorad, Milan, Italy), with a reference wavelength set at 655 nm. Cell viability was calculated as % ratio between the absorbance of cells treated with a sample and the absorbance of the cells kept in contact with the control, GM.

Proliferation test

In each well of a 96-well plate, 2×10^4 fibroblasts/well were seeded and grown 24 h to obtain subconfluence. Afterwards, cell substrates were put in contact with 200 µL of each sample. Nanoparticle suspensions and nanoparticle suspensions containing 5% w/w pull, as described in the section Lipid nanoparticle preparation, were diluted with GM in a 1/100 w/w ratio. Cells kept in contact with GM were considered as positive control (standard growth conditions). After 48 h contact, an MTT test was performed as previously described.

Cell migration/proliferation assay for wound healing

The gap closure cell migration/proliferation assay was performed according to a previously described procedure.[21,22] The assay employs Petri µ-Dishes (35 mm, Ibidi, Giardini, Milan, Italy), which contain a special insert consisting of two cell chambers (growth area: 0.22 cm^2 each) divided by a septum (500±50 µm in width), intended to simulate a cell-free gap.

Fibroblasts were seeded in each chamber at 10^5 cells/cm^2 concentration and grown at confluence in standard conditions as previously described. After 24 h, cells reached confluence and the insert was removed displaying two areas of cell substrates divided by the gap. The cell substrates were put in contact with 200 µL of each sample. Nanoparticle suspensions and nanoparticle suspensions containing 5% w/w pull, as described in the section Lipid nanoparticle preparation, diluted with GM in a 1/100 w/w ratio were tested. Cells kept in contact with GM were considered as control. At prefixed times (0 and 48 h), microphotographs were taken to evaluate cell migration in the gap.

As fibroblasts are migrating cells, a Br deoxyuridine test was associated to in vitro wound healing test to identify cells that were in proliferating phase (S-phase) (positively green and blue stained) and filled the gaps.

In particular, this test enabled identification of cell proliferation properties by assessing 5-bromo-2′-deoxyuridine (BrdU) incorporation in DNA synthesis. To this aim, in the last hour of culture, cells were labeled by adding 30 mM BrdU (Sigma-Aldrich) to the medium; then cells were washed with PBS and fixed in 70% ethanol. The incorporation of BrdU was detected by an immunostaining reaction with anti-BrdU antibody (Amersham Bioscience, VWR) as follows: the substrates were washed with PBS and incubated with HCl 2N for 30 min at room temperature. Cells were neutralized in 0.1 M sodium tetraborate (pH 8.5) for 15 min, washed twice for 5 min in PBS, and incubated for 20 min in a blocking solution, consisting of 1% w/v bovine serum albumin (Sigma-Aldrich) and 0.02% w/v Tween 20 (Sigma-Aldrich) in PBS. Cells were then incubated for 1 h with mouse anti-BrdU antibody, diluted 1:100 w/v in blocking solution, washed 3 times (10 min each) with the same solution and then incubated for 30 min in blocking solution containing anti-mouse immunoglobulin G fluorescein isothiocyanate-antibody (1:100 w/v dilution, Sigma-Aldrich). Finally, cell substrates were again extensively washed with PBS, counterstained for DNA with 0.5 mg/mL Hoechst 33258 (Sigma-Aldrich), and mounted in Mowiol (Sigma-Aldrich). Cells characterized by positive BrdU immunofluorescence were counted by using a fluorescence microscope (Zeiss Axiophot, Carl Zeiss, Jena, Germany).

Antimicrobial properties

The antimicrobial properties of nanoparticles and eucalyptus EO dispersed in lecithin solution at the same concentration of nanoparticles were assessed against the following reference bacterial strains: *Staphylococcus aureus* ATCC 6538 and *Streptococcus pyogenes* ATCC 19615. Before testing, bacteria were grown overnight in Tryptone Soya Broth (Oxoid, Thermo Fisher Scientific, Milan, Italy) at 37°C and in Todd Hewitt Broth (Oxoid, Thermo Fisher Scientific) at 37°C in the presence of 5% CO_2 in the case of *Streptococcus pyogenes*. The cultures were centrifuged at 224 *g* for 20 min, to separate microorganisms from culture broth and then washed with sterile distilled water. Washed cells were resuspended in Dulbecco's PBS and optical density at 650 nm wavelength was adjusted to 0.2, corresponding approximately to 1×10^7–1×10^8 colony-forming units/mL. The antimicrobial activity was determined with the macrodilution broth method, according to Clinical and Laboratory Standards Institute guidelines (2009), with some modifications. The desired sample concentration was achieved by adding in 15×100 mm test tubes an appropriate sample volume (nanoparticle suspension, as described in the section Lipid nanoparticle preparation) to 1 mL of double-concentrate isoSensitest broth (Oxoid, Thermo Fisher Scientific, Milan, Italy). Bacterial suspensions were added to the test tubes. The minimum inhibitory concentration (MIC) was evaluated after 24 h incubation at 37°C as the lowest concentration that completely inhibited the formation of visible microbial growth. Control test tubes contained microorganisms in culture broth without nanoparticles. Various concentrations of each sample were tested.

In vivo wound healing efficacy in rat model

All experiments on animals were carried out in full compliance with the standard international ethical guidelines (European Communities Council Directive 86/609/EEC), approved by Italian Health Ministry (D.L. 116/92). The study protocol was approved by the Local Institutional Ethics Committee of the University of Pavia for the use of animals. Male rats (Wistar 200–250 g) were anesthetized with equitensine at 3 mL/kg (39 mM pentobarbital, 256 mM chloral hydrate, 86 mM $MgSO_4$, 10% ethanol v/v, and 39.6% propyleneglycol v/v) and shaved to remove all hair from their backs. Three circular full-thickness burns, having a diameter of 4 mm, were produced on the back of the animals by contact with an aluminum rod (105°C for 40 s). Twenty-four hours later, the formed blisters were removed using a 4-mm diameter biopsy punch to obtain full-thickness lesions. Either 20 µL of nanoparticles suspension or 20 µL of nanoparticles suspension containing 5% w/w pull as described in the section Lipid nanoparticle preparation, was applied to the lesions. Lesions treated with 20 µL of saline solution were considered as control. After treatment, each lesion was protected with a sterile gauze and the rat's back was wrapped with a surgery

stretch (Safety, Bovisio Masciago, Italy). At prefixed times after blister removal (0, 3, 7, 10, 14, and 18 days), photographs of the lesions were taken by a digital camera (Sigma SD 14, Sigma Corporation, Milan, Italy), which allowed sizing of the lesions and monitoring the healing process. Each treatment was repeated after each photograph. The dimensions of wounded area were determined by an image analysis software (ICY, Institute Pasteur, Paris, France).

Histologic analysis

After 18th day treatment, the animals were killed, full-thickness biopsies were made in correspondence of the lesion area, and histologic analysis of the excised tissues was performed. A biopsy of intact skin was also taken for comparison. Tissue samples were bisected along the widest line of the wound, fixed for 48 h in 4% w/v neutral buffered paraformaldehyde, dehydrated with gradient ethanol series, cleared in xylene, and embedded in paraffin. Sections (8 µm) were obtained using a Leitz microtome (Wetzlar, Germany) and were stained with hematoxylin and eosin (H&E). The slices were examined at 5× magnification under a light microscope (Zeiss Axiophot, Carl Zeiss, Jena, Germany), equipped with a digital camera.

Statistical analysis

Statistical differences were evaluated by means of one-way analysis of variance (ANOVA) followed by multiple range test (Stat Graphics 5.0, Statistical Graphics Corporation, MD, USA). Differences were considered significant at $p<0.05$ level.

Results and discussion

Physical–chemical characterization of nanoparticles

Figure 1A and B reports the PS and PI of all lipid nanoparticles developed as a function of storage time (2°C–8°C). Figure 1A shows the results of SLN and NLC loaded with eucalyptus oil (e) or rosemary oil (r) and prepared by using olive oil (o), as liquid lipid, while Figure 1B shows the results of analogous nanosystems containing sesame oil (s), as liquid lipid.

Independent of nanoparticle composition, PS ranged from 220 to 300 nm and remained almost constant up to 3 months of storage. Similar results were obtained for PI that was close to 0.5, indicating nanoparticle populations characterized by a quite wide PS distribution, stable up to 3 months.

Bioadhesion properties

Figure 2 shows the normalized bioadhesion parameter (ΔAUC/AUC) of all the nanosystems developed, nanoparticles suspension and nanoparticles suspension containing 5% w/w pull.

Pull was characterized by good bioadhesive properties. Although all nanoparticles were stabilized lecithin and it is conceivable that their surface was coated by the same lecithin layers, different bioadhesion properties were observed.

Both SLN systems, either loaded with eucalyptus oil or with rosemary oil, were characterized by scarce bioadhesive properties. This result could be attributable to rigid structure

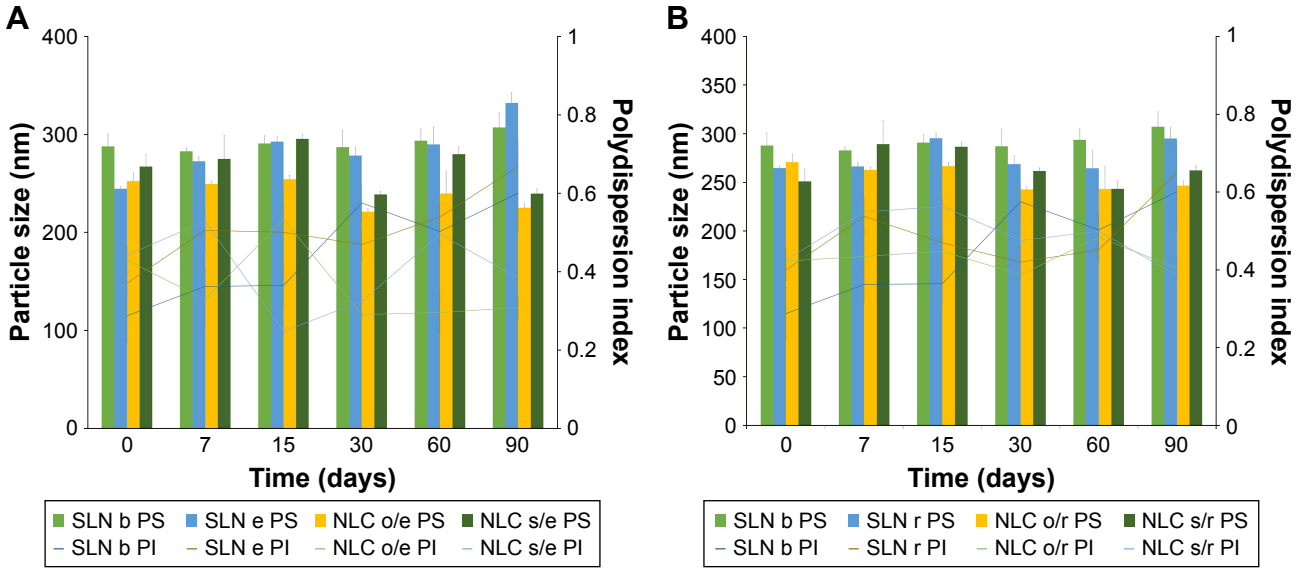

Figure 1 PS and PI as a function of storage time (2°C–8°C).
Notes: SLN and NLC prepared by using both eucalyptus oil or rosemary oil and (**A**) olive oil or (**B**) sesame oil as liquid lipids (mean value ± SD; n=6).
Abbreviations: SLN, solid lipid nanoparticles; NLC, nanostructured lipid carriers; b, blank-unloaded; e, eucalyptus oil; r, rosemary oil; o, olive oil; s, sesame oil; PI, polydispersity index; PS, particle size.

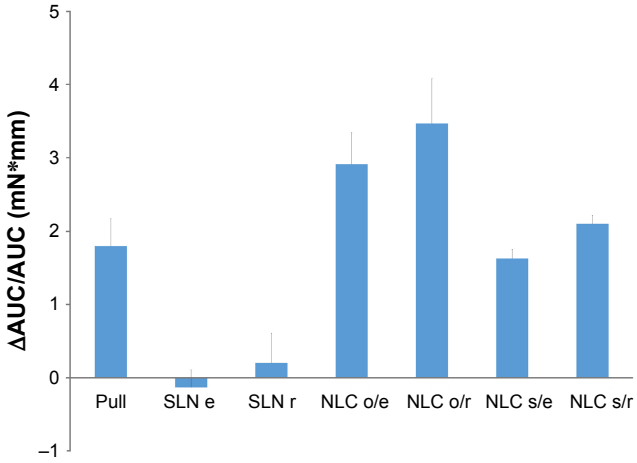

Figure 2 Bioadhesion parameter (normalized work of adhesion [ΔAUC/AUC]) of all the nanosystem suspensions and nanosystem suspensions containing 5% w/w pullulan (pull) (mean value ± SD; n=6).
Abbreviations: SLN, solid lipid nanoparticles; NLC, nanostructured lipid carriers; e, eucalyptus oil; r, rosemary oil; o, olive oil; s, sesame oil.

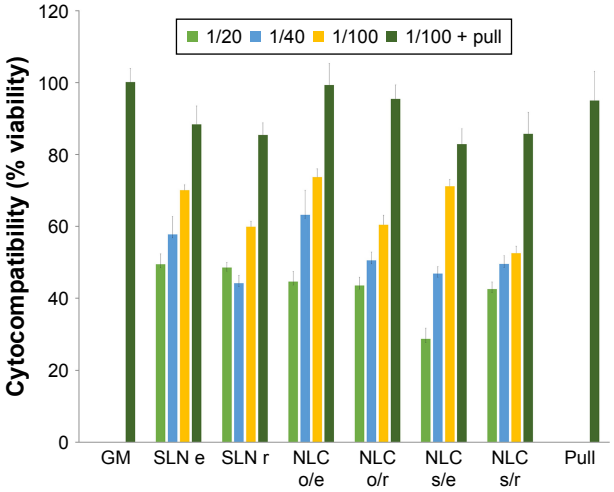

Figure 3 Cytocompatibility (viability %) of fibroblasts with all the nanoparticle suspensions, loaded with eucalyptus or rosemary oils (1/20, 1/40, and 1/100).
Notes: Nanoparticle suspensions containing 5% w/w pullulan were also tested at 1/100 dilution. GM was used as comparison (positive control) (mean value ± SD; n=8).
Abbreviations: e, eucalyptus oil; GM, growth medium; NLC, nanostructured lipid carriers; o, olive oil; r, rosemary oil; s, sesame oil; SLN, solid lipid nanoparticles.

of these nanoparticles, which impaired their interaction with the biologic substrates, preventing the formation of the bioadhesive joint. On the contrary, all NLC formulations were characterized by good bioadhesive properties. The systems containing olive oil showed bioadhesion parameters significantly higher than those of the corresponding systems prepared by using sesame oil (one-way ANOVA, multiple range test $p<0.05$).

Olive oil contains 85% of unsaturated fatty acids, in particular 70% of monounsaturated (mainly oleic and palmitoleic acid) and about 15% of polyunsaturated ones (mainly linoleic and linolenic acid). On the contrary, sesame oil contains about 85% unsaturated acids; mono- and poly-unsaturated acids, which are present in comparable amounts (41% of polyunsaturated – linoleic acid and 39% of monounsatured – oleic acid).

These differences in composition could determine a different lipid packaging in nanoparticle core and a consequent modification of NLC flexibility. This could cause a different degree of interaction with the biologic substrate and consequently a different strength of the bioadhesive joint.[23,24] Bioadhesion is an important property to assure efficacy, because it allows an intimate contact between wounded area and formulation.

In vitro biocompatibility properties

In Figure 3, cytocompatibility (% viability) of all the nanosystems developed, loaded with eucalyptus or rosemary oil, are compared. All the nanosytems (independent of the EO loaded) were characterized by concentration-dependent cytocompatibility. For a given formulation, the higher nanoparticle concentration (corresponding to the lowest dilution, 1/20) was characterized by % viability ranging from 30% to 50%, not significantly different than that of 1/40 dilution. On the contrary, 1/100 dilution determined a % viability ranging from 50% to 95%, significantly higher than those of the other two dilutions (one-way ANOVA, multiple range test $p<0.05$). The presence of pull determined an increase in cytocompatibility. NLC systems based on olive oil and containing 5% w/w pull were characterized at 1/100 dilution by cytocompatibility not significantly different than that of GM and significantly higher than those of NLC containing sesame oil (one-way ANOVA, multiple range test $p<0.05$).

Proliferation properties

Proliferation (% viability) results of all the nanosystems developed, loaded with eucalyptus or rosemary oil, are reported in Figure 4. Nanoparticles suspension and nanoparticles suspension containing 5% w/w pull were diluted at 1/100 and their proliferation properties compared. The nanosystems were characterized by proliferation properties not significantly different than those of the control (GM). In comparison with GM, 5% w/w pull solution (dilution 1/100) was able to significantly enhance cell proliferation. All nanosystems containing 5% w/w pull solution were characterized by a relevant improvement of proliferation properties; with the exception of NLC s/e, based on sesame oil and loaded with eucalyptus oil, all nanoparticles determined an enhancement of cell growth significantly higher than

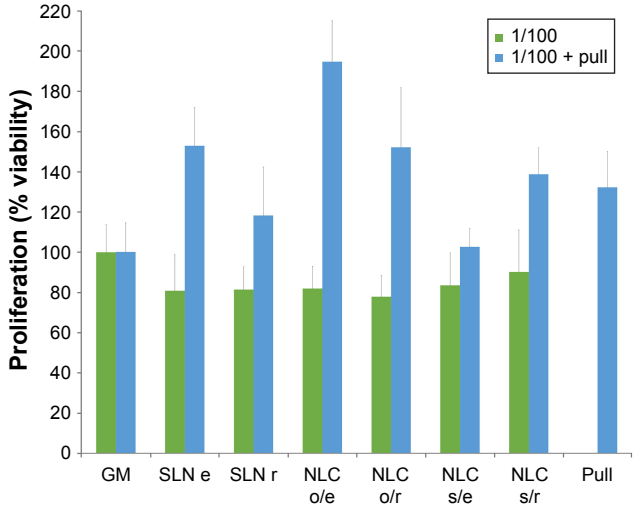

Figure 4 Proliferation (% viability) for all the nanosystems developed loaded with eucalyptus or rosemary oils.
Notes: Nanoparticle suspensions and nanoparticle suspensions containing 5% w/w pullulan at 1/100 dilution were tested. GM was used as comparison (positive control) (mean value ± SD; n=8).
Abbreviations: GM, growth medium; SLN, solid lipid nanoparticles; NLC, nanostructured lipid carriers; e, eucalyptus oil; r, rosemary oil; o, olive oil; s, sesame oil.

that of standard growth conditions (control, GM) (one-way ANOVA, multiple range test $p<0.05$). NLC o/e, based on olive oil and loaded with eucalyptus oil, was characterized by the best performance in terms of proliferation enhancement properties.

The presence of olive oil seems to favor cell proliferation: this result could be due to the high content of oleic acid, a fatty acid previously described for its good proliferation properties:[25] in fact the content of oleic acid is almost twofold greater than that of sesame oil.

Cell migration/proliferation properties in an in vitro wound healing test

Figure 5 reports the microphotographs of cell substrates taken at time 0 (immediately after insert removal) and after 48 h growing, by using an optical microscope or a fluorescence microscope (cell nuclei stained with Hoechst 33258 in blue and proliferating cells stained with anti-BrdU antibody in green).

All the samples were able to promote cell migration/proliferation in the gaps at least as the GM. In particular, cell substrates put in contact with NLC o/e, based on olive oil and loaded with eucalyptus oil, containing 5% w/w pull, showed a complete gap closure within 48 h after insert removal and a cell concentration higher than that of standard growth condition (control, GM). This nanosystem, therefore, demonstrated to be more effective in promoting wound healing in vitro.

The contact with NLC o/e determined a higher concentration of green-stained cells in the gap, that were proliferating cells, with respect to the other nanosystems. It is conceivable that oleic acid determined a synergic effect with eucalyptus oil to enhance cell proliferation. Given these results, NLC o/e was chosen as the most promising nanosystem and subjected to further characterization.

In vitro characterization of NLC o/e

Figure 6 reports the TEM microphotograph of NLC o/e. Nanoparticles were round shaped and showed a relatively small size dispersion around 50–60 nm, smaller than that expected on the basis of PCS measurements, which were probably affected by the presence of aggregates, responsible for a high PI (close to 0.5).[26] NLC o/e was characterized by a highly negative zeta potential equal to –22.07±0.29 mV (mean value ± SD, n=3). These results should conceivably be due to the presence onto nanoparticle surface of lecithin, which was proved to confer a negative zeta potential to nanosystems.[27] The presence of lecithin allowed particle stabilization and controlled particle aggregation as evidenced by 3-month stability results (Figure 1A and B). Eucalyptus EO loaded in NLC o/e was close to 100% (101.74±9.06%, mean value ± SD, n=3), indicating that the preparation procedure did not impair oil stability and loading, although it is a volatile extract.

Pure cocoa butter melting starts at 31°C and is completed at 34°C. After cutaneous application, given that skin temperature is 32°C, melting of the lipid core was conceivably the mechanism enabling the release of eucalyptus EO.

The MIC values measured against *Staphylococcus aureus* and *Streptococcus pyogenes* for NLC o/e and for eucalyptus EO, at the same EO concentration, are reported in Table 2.

Eucalyptus oil was characterized by the same MIC value (3 mg/mL) against *Staphylococcus aureus*, either as a free oil or after loading into NLC, indicating that encapsulation did not impair its antimicrobial activity. On the contrary, it showed an enhanced antimicrobial activity against *Streptococcus pyogenes* when encapsulated in NLC, because MIC values decreased from 1.5 mg/mL, for free oil, to 0.75 mg/mL, for NLC o/e.

In vivo wound healing efficacy of NLC o/e

Figure 7 reports the profiles of wound area (cm^2) as function of time. All the wounds treated with NLC o/e, as either nanoparticle suspension or nanoparticle suspension containing 5% w/w pull, and with saline solution (control) showed similar lesion area vs time profiles. After 4 days of treatment,

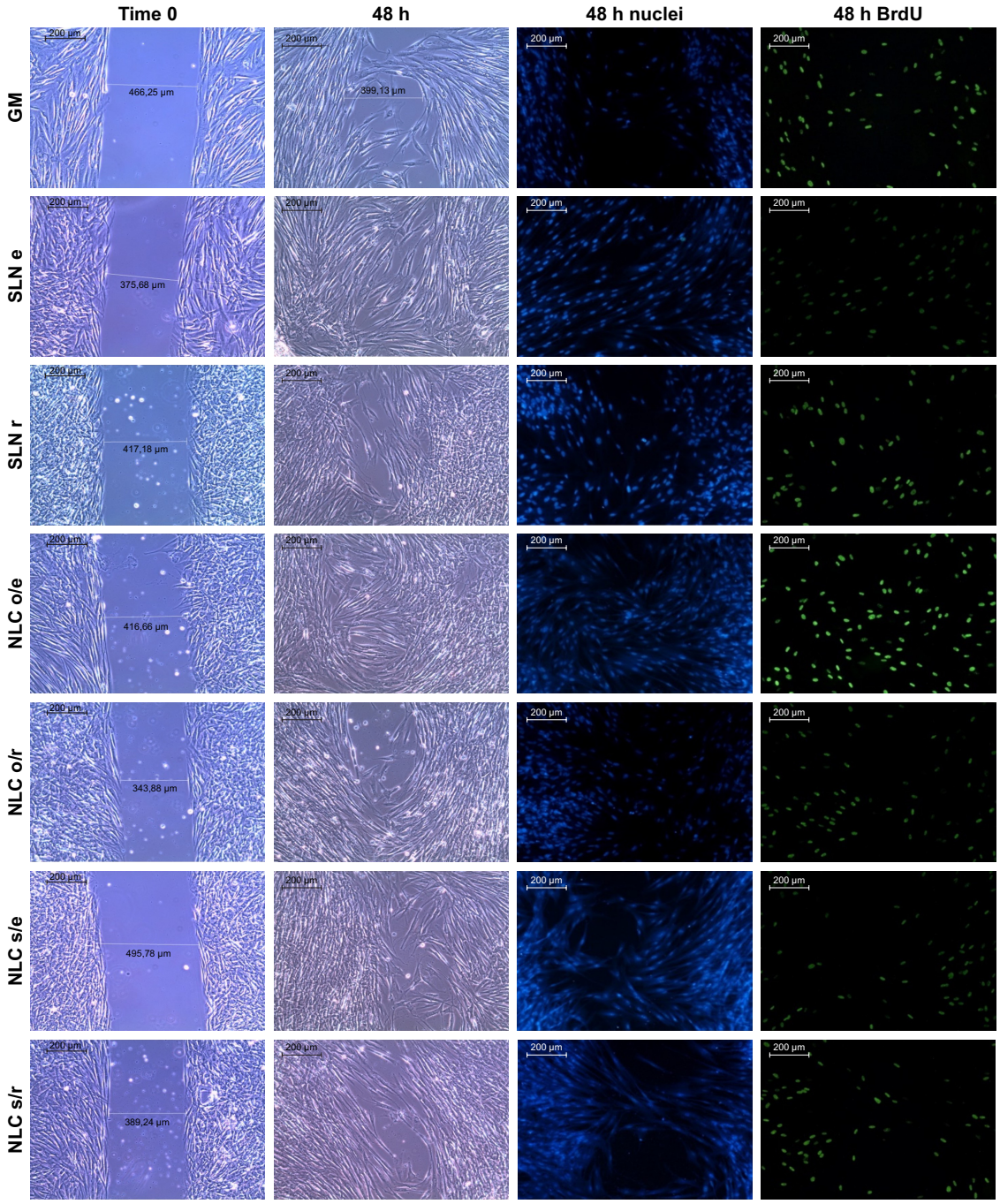

Figure 5 Microphotographs of cell substrates taken at time 0 (immediately after insert removal) and after 48 h of growth, by using optical microscope and after 48 h of growth by using fluorescence microscope (cell nuclei stained with Hoechst 33258 in blue and proliferating cells stained with anti-BrdU antibody in green). Scale bars =200 µm.
Abbreviations: GM, growth medium; SLN, solid lipid nanoparticles; NLC, nanostructured lipid carriers; e, eucalyptus oil; r, rosemary oil; o, olive oil; s, sesame oil.

NLC o/e suspension showed a significantly lower lesion area (not significantly greater than time 0) with respect to NLC o/e containing pull and saline solution, which were characterized by significantly greater dimensions than time 0 (one-way ANOVA, multiple range test $p<0.05$). At the 7th and 10th day of treatment both the lesions treated with NLC o/e, as either nanoparticle suspension or as nanoparticle suspension containing pull, presented dimensions not significantly different from each other and significantly lower than the lesion treated with saline solution (one-way ANOVA, multiple range test $p<0.05$). At the 15th day of treatment NLC o/e suspension presented the highest lesion reduction (one-way ANOVA, multiple range test $p<0.05$) indicating the capability of these nanoparticles to speed up tissue repairing. Given

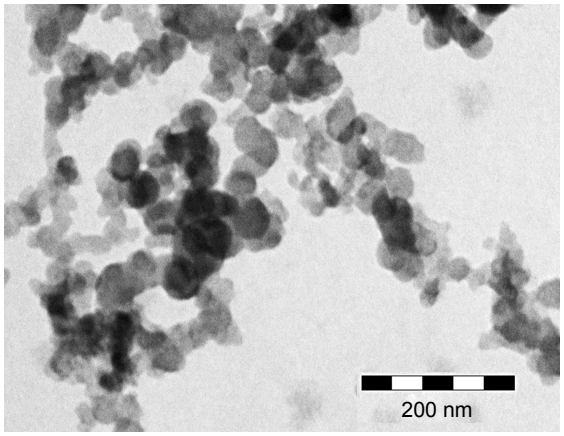

Figure 6 Transmission electron microscope microphotograph of NLC o/e.
Abbreviations: NLC, nanostructured lipid carriers; e, eucalyptus oil; o, olive oil.

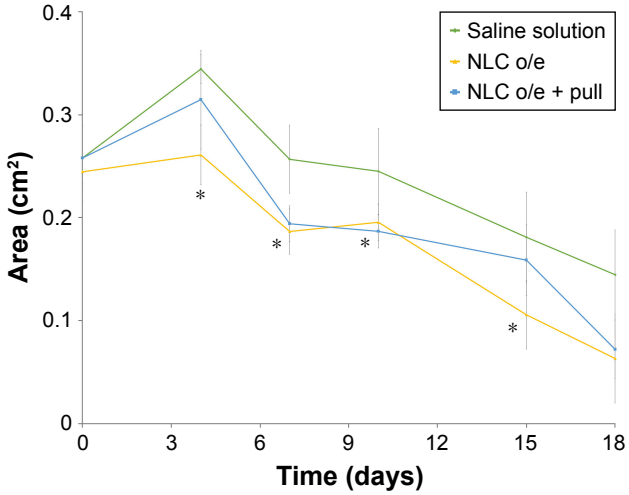

Figure 7 Profiles of wound area (cm^2) vs time profiles of wounds treated with NLC o/e suspension and NLC o/e suspension containing 5% w/w pullulan and saline solution (control) (mean value ± SD; n=3). *$p<0.05$, one-way ANOVA, multiple range test.
Abbreviations: NLC, nanostructured lipid carriers; e, eucalyptus oil; o, olive oil.

the high variability of results, such a difference could not be observed at 18th day of treatment.

Figure 8 reports microphotographs of skin sections of the wound area, stained with H&E, taken at the 18th day of treatment with saline solution (A), NLC o/e suspension (B), and NLC o/e suspension containing pull (C). Microphotograph of intact skin (D) is reported for comparison.

In correspondence with the wound treated with saline solution (control) (Figure 8A), a large part of epidermis was replaced by an eosinophil necrotic tissue (asterisk), and in the peripheral regions of the lesion, epidermis (bracket) was visible. In the underlying dermal connective tissue, an abundant granulation tissue (arrow) was present; moreover, collagen fibers were dispersed and not yet organized in large bundles, typical of the reticular layer of the dermis. There was no evidence of skin appendages (hair follicles and glands), while there were numerous vacuoles of different size (black star), delimited by a wall consisting of a monolayer of flattened cells (endothelium), probably corresponding to dilated vessels.

In correspondence with the wound treated with NLC o/e suspension (Figure 8B), epidermis (bracket) appeared continuous and well organized in multiple cell layers with a fair degree of keratinization. In the underlying connective tissue, skin appendages were vacant, but dermal papillae (white star) began to reform. A mild inflammatory infiltrate was visible (arrow), as well as a number of blood vessels (black star). Some scattered collagen fibers were present at the border with epidermis, while in the reticular layer of the dermis, the typical large bundles of collagen (white arrow) were already formed.

Table 2 MIC values against *Staphylococcus aureus* and *Streptococcus pyogenes* for eucalyptus essential oil and NLC o/e

	Strain	MIC (mg/mL)
Eucalyptus oil	*Staphylococcus aureus* ATCC 6538	3
	Streptococcus pyogenes ATCC 19615	1.5
NLC o/e	*Staphylococcus aureus* ATCC 6538	3
	Streptococcus pyogenes ATCC 19615	0.75

Abbreviations: ATCC, American Type Culture Collection; MIC, minimum inhibitory concentration; NLC, nanostructured lipid carriers; e, eucalyptus oil; o, olive oil.

In correspondence with the wound treated with NLC o/e suspension containing 5% w/w pull (Figure 8C), skin appeared completely re-epithelized, and epidermis (bracket) was well organized in multiple cell layers, with a fair degree of keratinization, similar to the structures observed in the section obtained from wound treated with NLC o/e (Figure 8B). Dermal papillae (white star) were in developing phase; furthermore, granulation tissue (arrows) and dilated vessels (black star) were present in a limited area, while collagen fibers were organized in large bundles, typical of the reticular layer of the dermis (white arrow).

Normal skin (Figure 8D) was characterized by epidermis (bracket), well organized in multiple cell layers, with a fair degree of keratinization and showed numerous dermal papillae (white star). Dermal layer was characterized by large bundles of collagen fibers (white arrow) and showed a lot of dermal appendages (white triangle), such as sebaceous glands and hair bulbs.

In summary, NLC e/o suspension containing pull promoted an excellent healing, with a good re-epithelization and stratum corneum formation. Although in the underlying connective tissue, skin appendages were vacant, collagen fibers were organized in large bundles typical of the reticular layer

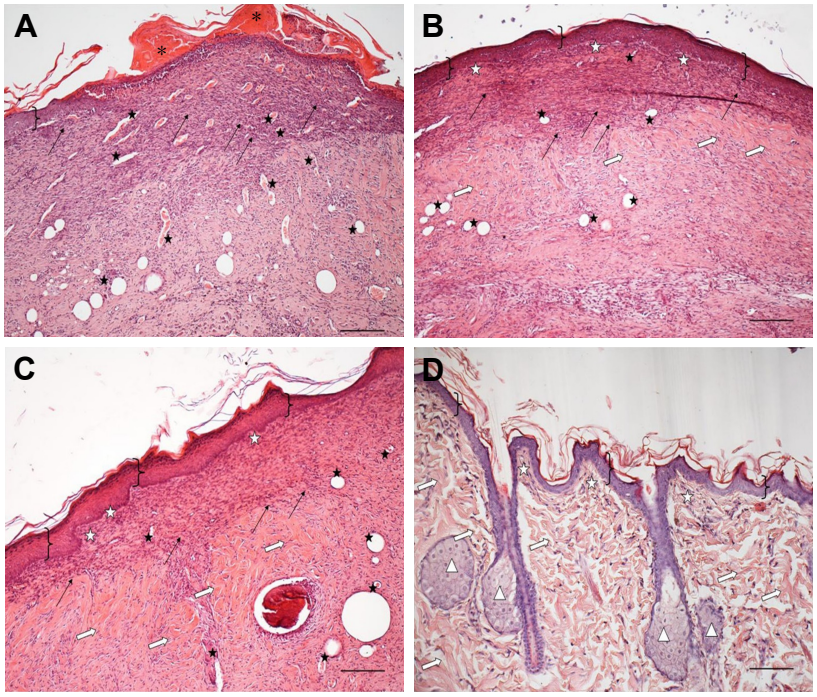

Figure 8 Microphotographs of skin sections stained with hematoxylin and eosin, taken from the wounded area at 18th day of treatment with saline solution, as negative control (**A**), nanostructured lipid carriers (NLC) o/e suspension (**B**), and NLC o/e suspension containing 5% w/w pullulan (**C**) in comparison with intact skin (**D**) (scale bar: 200 μm).
Notes: Asterisk: necrotic tissue; arrow: granulation tissue; black star: vacuoles/blood vessels; white star: dermal papillae; white arrow: bundles of collagen; white triangle: dermal appendages.
Abbreviations: NLC, nanostructured lipid carriers; e, eucalyptus oil; o, olive oil.

of the dermis. Moreover, dermal papillae began to reform. There was only a mild inflammatory infiltrate, visible in a small portion in the center of the wound.

Conclusion

NLC based on cocoa butter and olive oil, as solid and liquid lipids, respectively, and loaded with eucalyptus oil (NLC o/e) were prepared by high shear homogenization and ultrasound method. Lecithin was used as surfactant to stabilize nanoparticles and to avoid their aggregation. NLC o/e was characterized by a PS of 200–300 nm and demonstrated to be physically stable up to 3 months (2–8°C). It showed good bioadhesive properties, probably determined by NLC flexibility, which could promote interaction with the biologic substrate and the consequent bioadhesive joint formation; this is an important feature to allow an intimate contact between formulation and lesion, to assure treatment efficacy. NLC o/e showed good biocompatibility and proliferation properties toward normal human fibroblasts in an in vitro wound healing model. These properties could be due to the presence of olive oil, a fatty acid with a high content of oleic acid, already known for its good proliferation enhancement potential.

Encapsulation of eucalyptus oil in NLC did not impair its antimicrobial properties against two gram-positive bacterial strains commonly present in the skin (*Staphylococcus aureus* and *Streptococcus pyogenes*).

The results of in vivo rat burn model represented a proof of concept of efficacy and safety of NLC o/e developed.

Acknowledgments

Dr F Saporito wishes to thank ABOCA Società Agricola S.p.A. for supporting her PhD grant. The authors wish to thank Dr F Riva for performing the bromodeoxyuridine (BrdU) test and Dr M Boiocchi (Centro Grandi Strumenti, University of Pavia) for TEM images.

Disclosure

The authors report no conflicts of interest in this work.

References

1. Gould L, Abadir P, Brem H, et al. Chronic wound repair and healing in older adults: current status and future research. *J Am Geriatr Soc*. 2015; 63(3):427–438.
2. Boateng J, Catanzano O. Advanced therapeutic dressing for effective wound healing-review. *J Pharm Sci*. 2015;104(11):3653–3680.
3. Stejskalova A, Almquist BD. Using biomaterials to rewire the process of wound repair. *Biomater Sci*. 2017;5(8):1421–1434.

4. Gardner SE, Hillis SL, Heilmann K, Segre JA, Grice EA. The neuropathic diabetic foot ulcer microbiome is associated with clinical factors. *Diabetes*. 2013;62(3):923–930.
5. Bowler PG, Duerden BI, Armstrong DG. Wound microbiology and associated approaches to wound management. *Clin Microbiol Rev*. 2001; 14(2):244–269.
6. Jahromi MAM, Zangabad PS, Basri SMM, et al. Nanomedicine and advanced technologies for burns: preventing infection and facilitating wound healing. *Adv Drug Deliv Rev*. Epub 2017 Aug 4.
7. Fuzi M. Editorial: the global challenge posed by the multiresistant international clones of bacterial pathogens. *Front Microbiol*. 2017;8:817.
8. Davis SC, Perez R. Cosmeceuticals and natural products: wound healing. *Clin Dermatol*. 2009;27(5):502–506.
9. Mayaud L, Carricajo A, Zhiri A, Aubert G. Comparison of bacteriostatic and bactericidal activity of 13 essential oils against strains with varying sensitivity to antibiotics. *Lett Appl Microbiol*. 2008;47(3):167–173.
10. Ait-Ouazzou A, Loran S, Bakkali M, et al. Chemical composition and antimicrobial activity of essential oils of Thymus algeriensis, Eucalyptus globulus and Rosmarinus officinalis from Morocco. *Sci Food Agric*. 2011; 91(14):2643–2651.
11. Takahashi T, Kokubo R, Sakaino M. Antimicrobial activities of eucalyptus leaf extracts and flavonoids from Eucalyptus maculata. *Lett Appl Microbiol*. 2004;39(1):60–64.
12. Moss M, Cook J, Wesnes K, Duckett P. Aromas of rosemary and lavender essential oils differently affect cognition and mood in healthy adults. *Int J Neurosci*. 2003;113(1):15–38.
13. Apostolides NA, El Beyrouthy M, Dhifi W, et al. Chemical composition of aerial parts of Rosmarinus officinalis L. Essential oil growing wild in Lebanon. *J Essent Oil Bear Pl*. 2013;16(2):274–282.
14. Sienkiewicz M, Lysakowska M, Pastuszka M, Bienias W, Kowalczyk E. The potential of use basil and rosemary essential oils as effective antibacterial agents. *Molecules*. 2013;18(8):9334–9351.
15. Drulis-Kawa Z, Dorotkiewicz-Jach A. Liposomes as delivery systems for antibiotics. *Int J Pharmaceut*. 2010;387(1):187–198.
16. Gokce EH, Korkmaz E, Dellera E, Sandri G, Bonferoni MC, Ozer O. Resveratrol loaded solid lipid nanoparticles versus nanostructured lipid carriers: evaluation of antioxidant potential for dermal applications. *Int J Nanomed*. 2012;7:1841–1850.
17. Gokce EH, Korkmaz E, Tuncay-Tanrıverdi S, et al. A comparative evaluation of coenzyme Q10 loaded liposomes and solid lipid nanoparticles as dermal antioxidant carriers. *Int J Nanomed*. 2012;7:5109–5117.
18. Sandri G, Bonferoni MC, D'Autilia F, et al. Wound dressings based on silver sulfadiazine SLN for tissue repairing. *Eur J Pharm Biopharm*. 2013;84(1):84–90.
19. Szucs M, Sandri G, Bonferoni MC, et al. Mucoadhesive behaviour of emulsion containing polymeric emulsifier. *Eur J Pharm Sci*. 2008; 34(4):226–235.
20. Sandri G, Rossi S, Bonferoni MC, et al. Buccal penetration enhancement properties of N-trimethyl chitosan: influence of quaternization degree on absorption of a high molecular weight molecule. *Int J Pharm*. 2005;297(1):146–155.
21. Sandri G, Bonferoni MC, Ferrari F, et al. Montmorillonite-chitosan-silver sulfadiazine nanocomposites for topical treatment of chronic skin lesions: in vitro biocompatibility, antibacterial efficacy and gap closure cell motility properties. *Carbohyd Polym*. 2014;102:970–977.
22. Sandri G, Bonferoni MC, Rossi S, et al. Platelet lysate embedded scaffolds for skin regeneration. *Expert Opin Drug Del*. 2015;12(4): 525–554.
23. Yang Y, Corona A, Schubert B, Reeder R, Henson M. The effect of oil type on the aggregation stability of nanostructured lipid carriers. *J Colloid Interface Sci*. 2014;418:261–272.
24. Barauskas J, Christerson L, Wadsater M, Lindstrom F, Lindqvist A-K, Tiberg F. Bioadhesive lipid compositions: self-assembly structures, functionality and medical applications. *Mol Pharmceutics*. 2014;11(3): 895–903.
25. Dellera E, Bonferoni MC, Sandri G, et al. Development of chitosan oleate ionic micelles loaded with silver sulfadiazine to be associated with platelet lysate for application in wound healing. *Eur J Pharm Biopharm*. 2014;88(3):643–650.
26. Sandri G, Bonferoni MC, Gökçe EH, et al. Chitosan-associated SLN: in vitro and ex vivo characterization of cyclosporine A loaded ophthalmic systems. *J Microencapsul*. 2010;27(8):735–746.
27. Chibowski E, Szcześ A. Zeta potential and surface charge of DPPC and DOPC liposomes in the presence of PLC enzyme. *Adsorption*. 2016;22(4–6):755–765.